

Supplementary Information

Principal Component Analysis to Enhance Enantioselective Raman Spectroscopy

Claudia C. Rullich¹ and Johannes Kiefer^{1,2*}

¹Technische Thermodynamik, Universität Bremen, Badgasteiner Str. 1, 28359 Bremen,
Germany.

²MAPEX Center for Materials and Processes, Bibliothekstr.1, Universität Bremen, 28359
Bremen, Germany.

*Corresponding author. Phone: +49 421 218 64777. Email: jkiefer@uni-bremen.de

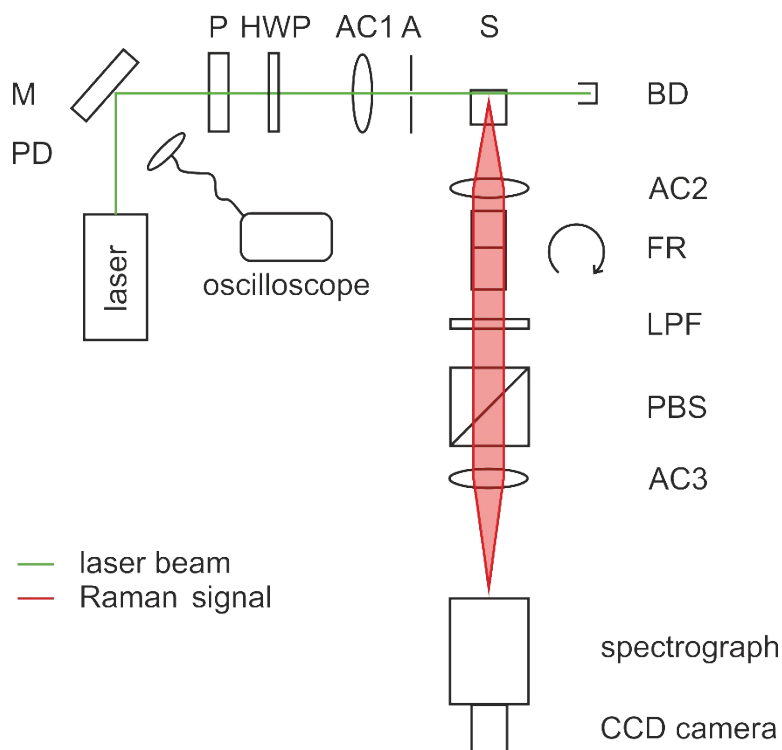


Fig. S1: Schematic of 90° enantioselective Raman set-up. A: aperture, AC: achromatic lens, BD: beam dump, FR: half-wave Fresnel rhomb, HWP: half-wave plate, LPF: longpass filter, M: mirror, P: polarizer, PD: photo diode, S: sample.

Tab. S1 Peak assignment for Raman and ATR-FTIR spectra of 4-methylpentan-2-ol: str.=stretching, def.=deformation, sciss.=scissoring, rock.=rocking, wagg.=wagging, tors.=torsion, s=symmetric, as=antisymmetric, sh=shoulder, FR=Fermi resonance.

Raman wavenumber /cm ⁻¹	FTIR wavenumber /cm ⁻¹	own assignment	Reference
338		CCC def.	1
353(sh)		CCO def., CCC def.	1
386		CCC def.	1
428		CCO def., CCC def.	1
442		CCO def., CCC def.	1
462		CCO def., CCC def.	1
489		CCO def., CCC def.	1
518		CCO def., CCC def.	1
780		CH ₂ rock.	1
818 (sh)		CC str.	1
826	826	(C) ₂ CO s str.	2
844 (sh)	846 (sh)	CH ₂ rock., CH ₃ rock.	1
878	880	CC str.	1

921	924	CC str., CH ₃ rock.	1
951		CC str., CH ₃ rock., CO str.	1
963		CC str., CH ₃ rock., CO str.	1
	972	CO str., CC str.	1
1012	1017	CO str., CH ₂ tors.	1
1039 (sh)		CO str., CH ₂ tors.	1
1049		CC str.	1
	1056	CO str., CC str.	1
1107 (sh)		CH ₃ rock.	1
	1115	CH ₂ rock.	1
1126 (sh)		CH ₂ rock.	1
		(C) ₂ CO as str.	2
1142	1140 (sh)	(C) ₂ CO as str.	2
1157 (sh)	1154	(C) ₂ CO as str.	2
	1169	(C) ₂ CO as str.	2
1224		CH ₂ rock., CH ₃ rock.	1
	1234	CH ₂ rock., CH ₃ rock.	1
	1275	CH ₂ wagg., COH def.	1
1308 (sh)	1312	COH def.	1
1325		CH ₃ s def.	3
	1332	CH ₃ s def.	3
	1345	CH ₃ s def.	3
	1370	CH ₃ s sciss. CH(CH ₃) ₂ sciss.	2 2
	1383 (sh)	CH(CH ₃) ₂ sciss.	2
	1413	CH ₂ sciss.	1
	1425 (sh)	CH ₂ sciss.	1
1433		CH ₂ sciss.	
1441		CH ₃ as def. CH ₃ as sciss.	3 2
	1459 (sh)	CH ₃ as sciss.	2
	1469	CH ₃ as def.	1
2713		Combination	1
	2724	Combination	1
2756		Combination	1
	2841 (sh)	Overtone	1
2875	2874	CH ₂ s str	1, 2
2894		CH ₂ s str., FR	2
2908 (sh)		CH ₂ s str.	1
	2920	CH ₂ FR	2
2931	2931 (sh)	CH ₃ s str	1
2964	2960	CH ₂ as str.	1
3360	3344	OH str.	1

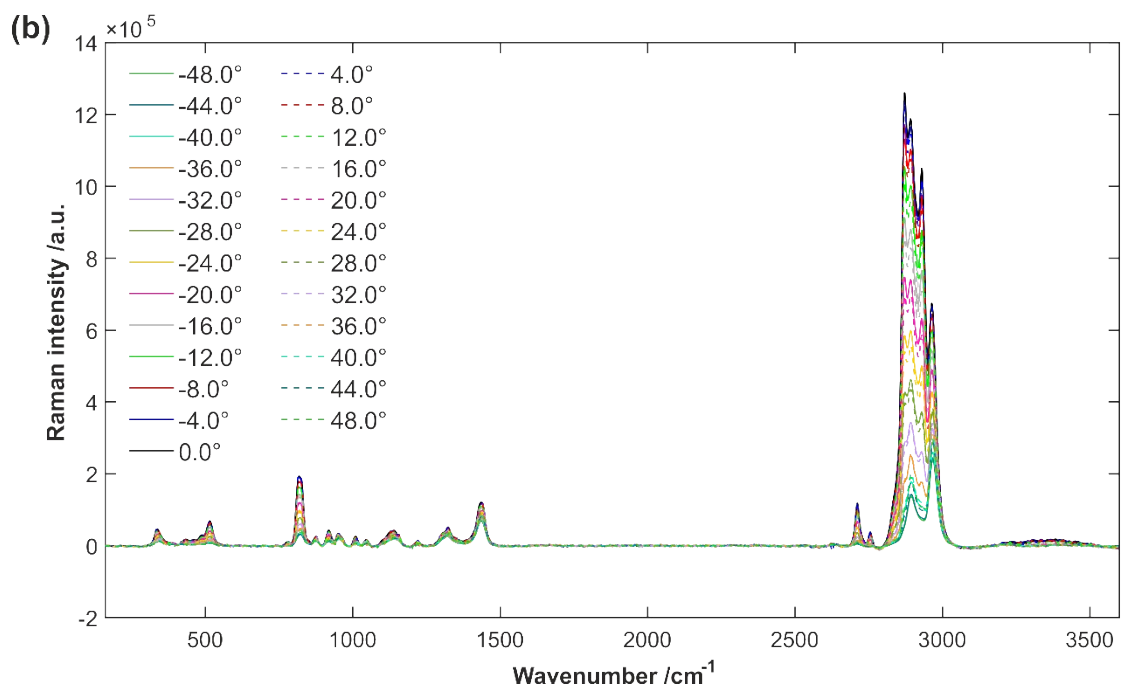
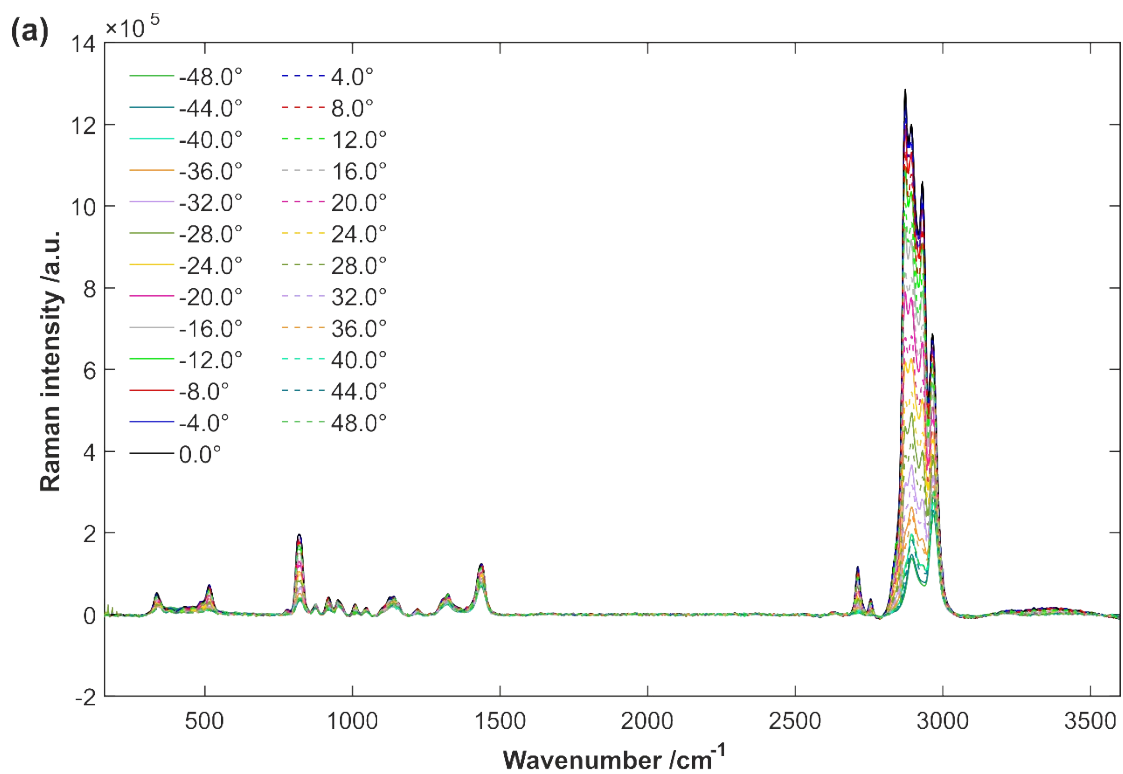


Fig. S2 Retarder-resolved Raman spectra of (2R)-(-)-4-methylpentan-2-ol (a) and (2R2S)-(+)-4-methylpentan-2-ol in the range $-48.0^\circ \leq \theta \leq 48.0^\circ$ in steps of 4.0° .

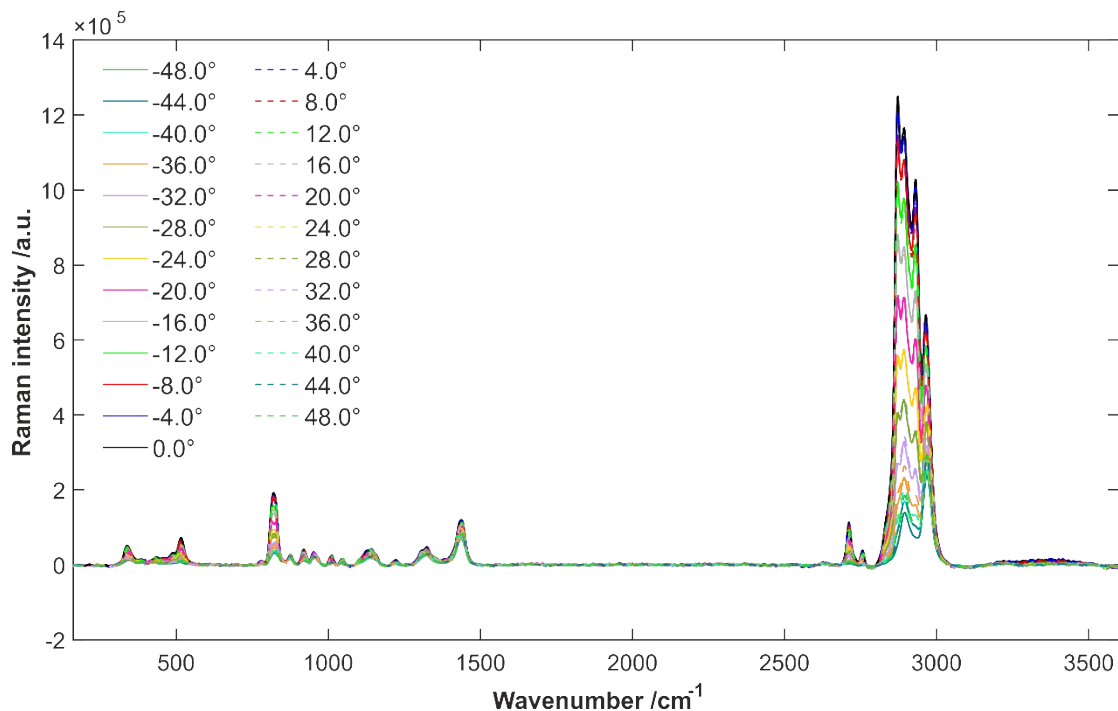


Fig. S3 Retarder-resolved Raman spectra of (2S)-(+)-4-methylpentan-2-ol in the range $-48.0^\circ \leq \theta \leq 48.0^\circ$ in steps of 4.0° .

The parameters in Tab. S2 are obtained using the esR spectra of (2R2S)-(\pm)-4-methylpentan-2-ol in Fig. S2 (b). The relative Raman intensities ΔI_{rel}^B of a medium B are calculated according to eq. (S1)-(S3) with one simplification. The depolarization ratio of a vibrational band is assumed to be equal for all three media, i.e. is independent of the optical rotation α . For a more accurate analysis, the depolarization ratio has to be calculated dependent on α .⁴

Tab. S2 Parameters for calculation of relative Raman intensity differences according to eq. (S1)-(S3).

Wavenumber /cm ⁻¹	Depolarization ratio	Amplitude A	Minimum Intensity I_{min}	$b_{rac} /^\circ$	$b_{(-)} /^\circ$	$b_{(+)} /^\circ$
2894	0.24	0.880	0.120	0.0	1.5	-1.5
2964	0.73	0.362	0.208	0.0	1.5	-1.5

The retarder-resolved intensity for a vibrational band (vib) at the angle of the half-wave retarder θ_i can be calculated according to eq. (S1) with the Amplitude A_{vib} , the minimum intensity $I_{min,vib}$ and the shift b of the maximum intensity along θ ($b=-\alpha$).

$$I_{vib}(\theta_i) = A_{vib} \cos^2(2\theta_i + b) + I_{min,vib} \quad (S1)$$

Normalizing the intensity of a vibrational band (vib1) with respect to the corresponding intensity of a vibrational band (vib2) with different symmetry delivers

$$I_{norm,vib2}^B(\theta_i) = I_{vib1}^B(\theta_i)/I_{vib2}^B(\theta_i) \quad (S2)$$

In a last step, the difference of the normalized intensity and a reference medium $I_{norm,vib2}^{ref}(\theta_i)$, e.g. the racemate, is calculated relatively to the reference medium

$$\Delta I_{rel}^B(\theta_i) = \frac{I_{norm,vib2}^B(\theta_i) - I_{norm,vib2}^{ref}(\theta_i)}{I_{norm,vib2}^{ref}(\theta_i)} \quad (S3)$$

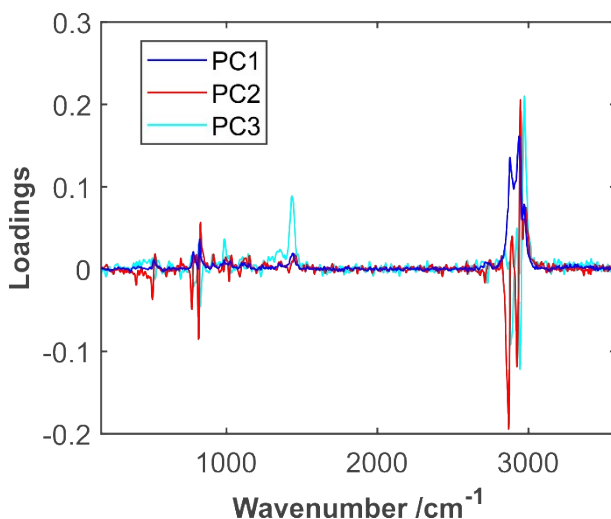


Fig. S4 Loadings of the first three components of the difference Raman spectra of the pure enantiomers of butan-2-ol. PCA conducted with spectra taken from the half-wave retarder angular range $-46^\circ \leq \theta \leq 46^\circ$.

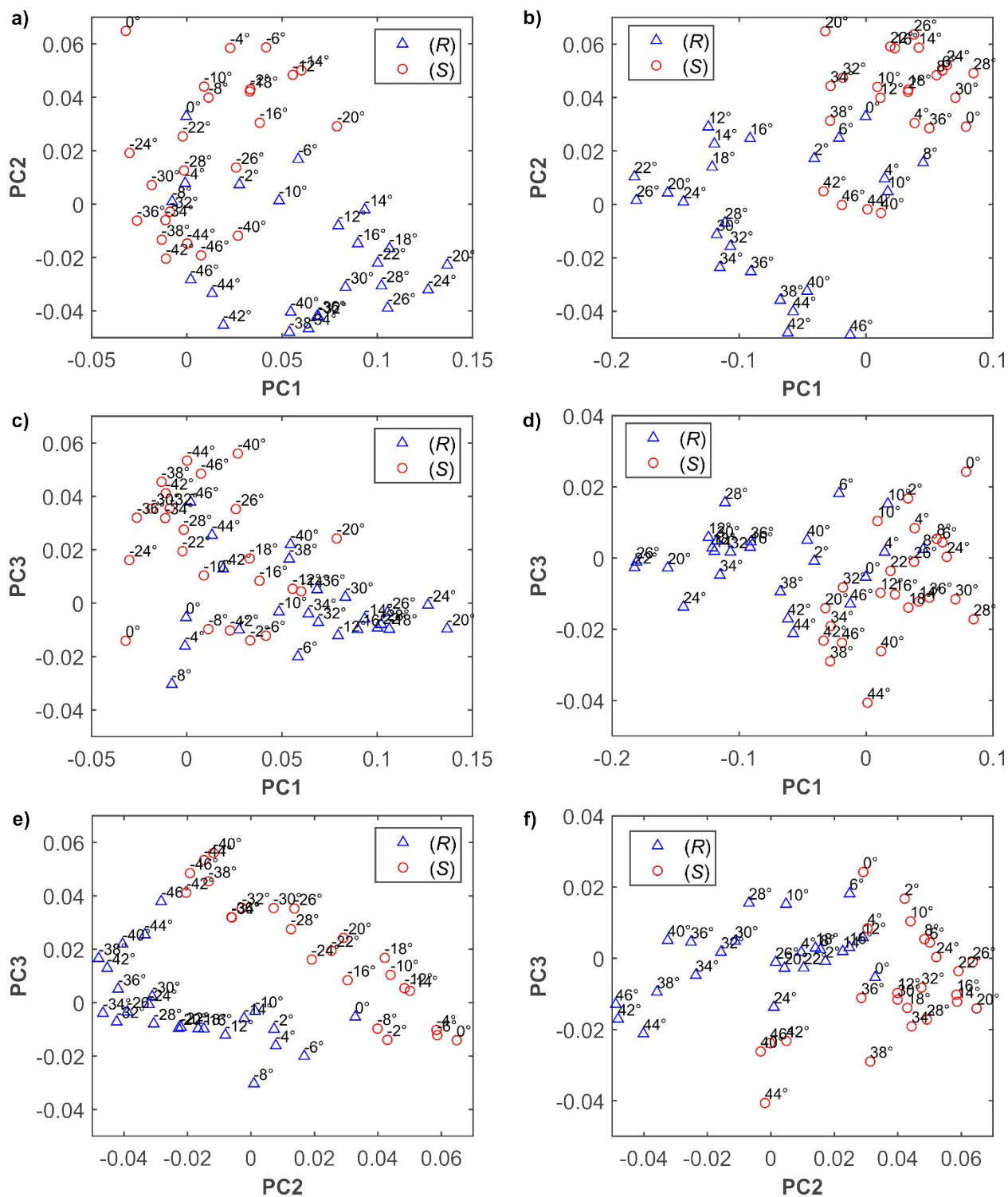


Fig.S5 Principal component analysis (scores) of difference spectra of the pure enantiomers of butan-2-ol with the explained variances of 57.2%, (PC1), 12.4% (PC2), and 5.2% (PC3). For clarity, the results of the analysis are split up into two angular ranges: $-46^\circ \leq \theta \leq 0^\circ$ in the left panel (a, c, e) and $0^\circ \leq \theta \leq 46^\circ$ in the right panel (b, d, f). EsR spectra are taken from previous measurements according to Ref.⁵.

References

1. J. Kiefer, S. Wagenfeld and D. Kerlé, *Spectrochim. Acta, Part A*, 2018, **189**, 57-65.
2. P. Larkin, *Infrared and Raman Spectroscopy: Principles and Spectral Interpretation*, Elsevier, Oxford, 2011.
3. G. Socrates, *Infrared and Raman Characteristic Group Frequencies: Tables and Charts*, John Wiley & Sons Ltd, Chichester, third edn., 2001.
4. J. Kiefer and M. Kaspereit, *Anal. Methods*, 2013, **5**, 797-800.
5. C. C. Rullich and J. Kiefer, *Analyst*, 2018, **143**, 3040-3048.